arXiv:0902.1506v3 [q-bio.GN] 20 May 2009

Needles in the Haystack: Identifying Individuals Present in Pooled Genomic Data

Rosemary Braun, William Rowe, Carl Schaefer
Jinghui Zhang, and Kenneth Buetow
National Cancer Institute, NIH, Bethesda, MD.

May 21, 2009

Abstract

Recent publications have described and applied a novel metric that quantifies the genetic distance of an individual with respect to two population samples, and have suggested that the metric makes it possible to infer the presence of an individual of known genotype in a sample for which only the marginal allele frequencies are known. However, the assumptions, limitations, and utility of this metric remained incompletely characterized. Here we present an exploration of the strengths and limitations of that method. In addition to analytical investigations of the underlying assumptions, we use both real and simulated genotypes to test empirically the method's accuracy. The results reveal that, when used as a means by which to identify individuals as members of a population sample, the specificity is low in several circumstances. We find that the misclassifications stem from violations of assumptions that are crucial to the technique yet hard to control in practice, and we explore the feasibility of several methods to improve the sensitivity. Additionally, we find that the specificity may still be lower than expected even in ideal circumstances. However, despite the metric's inadequacies for identifying the presence of an individual in a sample, our results suggest potential avenues for future research on tuning this method to problems of ancestry inference or disease prediction. By revealing both the strengths and limitations of the proposed method, we hope to elucidate situations in which this distance metric may be used in an appropriate manner. We also discuss the implications of our findings in forensics applications and in the protection of GWAS participant privacy.

1 Introduction

In the recently published article "Resolving Individuals Contributing Trace Amounts of DNA to Highly Complex Mixtures Using High-Density SNP Genotyping Microarrays" [1], the authors describe a method by which the presence of a individual with a known genotype may be inferred as being part of a mixture of genetic material for which marginal minor allele frequencies (MAFs), but not sample genotypes, are known.

The method [1] is motivated by the idea that the presence of a specific individual's genetic material will bias the MAFs of a sample of which they are part in a subtle but systematic manner, such that when considering multiple loci, the bias introduced by a specific individual can be detected even when his DNA comprises only a small fraction of the mixture. More generally, it is well known that samples of a population will exhibit slightly different MAFs due to sampling variance following a binomial distribution; the genotype of the individual in question contributes to this variation, and so may be "closer" to a sample containing him than to a sample which does not. Based on this intuition, the article [1] defines a genetic distance statistic to measure the distance of an individual relative to two samples, summarized as follows:

Consider an underlying population P from which two samples F (of size n_F) and G (of size n_G) are drawn independently and identically distributed (i.i.d.) [in [1], these are referred to as "reference" and "mixture" respectively]. Consider now an additional sample Y; we wish to detect whether Y was drawn from G, versus the null hypothesis that Y was drawn from P independent of G and F. Given the MAFs f_i and g_i at locus i for F and G, respectively, and given the MAFs y_i for sample Y with $y_i \in \{0, 0.5, 1\}$ (corresponding to homozygous major, heterozygous, and homozygous minor alleles) at each locus i, [1] defines the relative distance of sample Y from F and G at i as:

$$D_i(Y) = |y_i - f_i| - |y_i - g_i| \ . \tag{1}$$

By assuming only independent loci are chosen and invoking the central limit theorem for the large number of loci genotyped in modern studies, the article [1] asserts that the Z-score of D_i across all loci will be normally distributed,

$$T(Y) = \frac{\langle D_i \rangle - \mu_0}{\sqrt{\mathsf{Var}(D_i)/s}} = \frac{\langle D_i \rangle}{\sqrt{\mathsf{Var}(D_i)/s}} \sim N(0,1) \tag{2}$$

where $\langle \cdot \rangle$ denotes the average over all SNPs i, s is the number of SNPs, and Eq. 2 exploits the assumption [1] that an individual who is in neither F nor G will be on average equidistant to both under the null hypothesis, i.e., $\mu_0 = 0$. The article [1] proposes using this approach in a forensics context, in which G is a mixture of genetic material of unknown composition (e.g., from a crime scene), and Y is suspect's genotype; by choosing an appropriate reference sample for group F, it is hypothesized that large, positive T will be obtained for individuals whose genotypes are included in G, and hence bias g_i, while individuals whose genotypes are not in G should have insignificant T since they should intuitively be no more similar to the mixture sample G than they are to the reference sample F.

In [1], the authors applied this test to a multitude of individuals Y, each of which are present in the samples constructed by them for F or G, and report near-zero false negative rates. The article concludes that it is possible to identify the presence of DNA of specific individuals within a series of highly complex genomic mixtures, and that these "findings show a clear path for identifying whether specific individuals are within a study based on summary-level statistics." In response, many GWAS data sources have retracted the publicly available frequency data pending further

study of this method due to the concern that the privacy of study participants can be compromised. However, because no samples absent from both F and G were used, false positive rates—significant T for individuals neither in G nor F—are not assessed in practice; rather, they are simply assumed to follow the nominal false-positive rate α given by quantiles of the putative null distribution in Eq. 2.

In this manuscript, we expand on [1] by investigating the method's robustness to several inherent assumptions:

1. that F, G, and Y are all i.i.d. samples of the same population P and hence the difference of MAFs f_i and g_i in the two samples is small;

2. that the loci i are independent, such that the central limit theorem may be invoked in Eq 2; and

3. that an individual Y_- in neither G nor F does not have sufficient genotype identity (e.g., via inheritance) to true positive individual Y_+ that $D_i(Y_-) \approx D_i(Y_+)$ for enough i to bias $T(Y_-)$.

To investigate the effect of these assumptions, we begin with a statement of the problem that [1] attempts to address, analytically derive the effect of deviations from the assumptions, and empirically explore the accuracy of the method in practice using real and simulated genotype data. We conclude with a discussion of the implications of our findings, both in forensics as well as regarding identification of individuals contributing DNA in GWAS.

The results presented here reveal that membership classification via Eq. 2 is sensitive to the choice of F and G; that even a small amount of LD will alter the distribution of T for null samples; and that individuals who are related to members of F or G are frequently assigned significant T values. Our findings suggest that Eq. 2 will in practice yield a high false-positive rate if used to discern the membership of an individual in a specific sample, and when used for this purpose is likely be accurate only if the above assumptions are exceedingly well-met and the individual Y is believed *a priori* to be present in exactly one of F or G. However, although these findings suggest that Eq. 2 may have limited utility to reliably detect the identity of an individual in F or G without prior knowledge, it may be valuable for verifying that an individual is *not* in either sample, and we find some suggestion that the metric (Eq. 1) proposed in [1] could perhaps be extended to other genetic-similarity problems (e.g., in ancestry inference).

2 Materials and Methods

We explore the performance of the method described in [1] both analytically and empirically. For the empirical studies, we attempt to classify real and simulated samples into pools derived from publicly available data sources in order to assess the chances that an individual is mistakenly classified into a group which does not contain his specific genotype. The data used in these tests is described below:

2.1 Experimental genotypes and MAFs

Real-world genotypes from publicly available data sets were retrieved as follows: 2287 samples with known genotypes were obtained from the Cancer Genomic Markers of Susceptibility (CGEMS) breast cancer study. The samples were sourced as described in [2]. Briefly, the samples comprised 1145 breast cancer cases (sample group C+) and a comparable number (1142) of matched controls (group C–) from the participants of the Nurses Health Study. All the participants were American women of European descent. The samples were genotyped against the Illumnina 550K arrays, which assays over 550,000 SNPs across the genome. To assess the genetic identity shared between samples, we computed the fraction of SNPs with identical alleles for all possible pairs of individuals; none exceeded 0.62.

Additionally, 90 genotypes of individuals of European descent (CEPH) and 90 genotypes of individuals of Yoruban descent (YRI) were obtained from the HapMap Project [3]. In both cases, the 90 individuals were members of 30 family trios comprising two unrelated parents and their offspring. SNPs in common with those assayed by the CGEMS study and located on chromosomes 1–22 were kept in the analysis (sex chromosomes were excluded since the CGEMS participants were uniformly female); a total of 481,482 SNPs met these criteria.

Minor allele frequencies for case and control groups were computed from the CGEMS genotypes. Publicly-available minor allele frequencies from the 60 unrelated CEPH individuals were retrieved directly from the HapMap Project [3]. The distribution of MAF differences for each group may be seen in Fig. 1.

2.2 Simulated Genotypes I

To explore the potential for a sample whose genotype is drawn on f_i or g_i (without being a member of F or G) to be misclassified, five sets of 320 simulated genotypes were created by drawing a genotype for each SNP independently as a pair of Bernoulli trials from given allele frequencies:

S.1: For each locus in each sample, genotypes were drawn on the CGEMS control allele frequencies for that locus.

S.2: For each locus in each sample, genotypes were drawn on the CGEMS case allele frequencies for that locus.

S.3: For each locus in each sample, genotypes were drawn on the HapMap CEPH [3] allele frequencies for that locus.

S.4: For each sample, 50% of the loci were selected at random to have genotypes drawn on CGEMS case frequencies, and the other 50% had genotypes drawn on CGEMS control frequencies.

S.5: For each sample, 50% of the loci were selected at random to have genotypes drawn on HapMap CEPH frequencies, 25% of the the of the loci were selected at random to have genotypes drawn

on CGEMS case frequencies, and the other 25% had genotypes drawn on CGEMS control frequencies.

2.3 Simulated Genotypes II

To further explore the influence of genetic similarity, two other simulation sets were created. Beginning with the MAFs from CGEMS controls, here denoted by p_i, we create the first set as follows:

1. Draw f_i from $\mathsf{Bin}(2000, p_i)/2000$ to simulate the MAFs of a sample of 1000 individuals;
2. Draw 1000 genotypes on $\mathsf{Bin}(2, p_i)/2$ to simulate genotypes of 1000 individuals who will comprise G;
3. Construct 200 genotypes (Ys) for which q percent of SNPs are chosen at random to be identical to a specific G individual (selected at random for each of the 200 samples), and the other $1 - q$ fraction of SNPs are drawn on $\mathsf{Bin}(2, p_i)/2$;
4. Perform step 3 for values of q in 0.01 increments from 0 to 1, thus generating 100 pools of 200 samples each who bear q identity to a true-positive individual, and apply Eqs. 1,2 to classify them against the F and G generated in steps 1 and 2.

A second set is created as follows, also using the MAFs from CGEMS controls as p_i:

1. Draw f_i, g_i independently from $\mathsf{Bin}(2000, p_i)/2000$ to simulate the MAFs of two samples of 1000 individuals each;
2. Draw 200 genotypes (Ys) on $\mathsf{Bin}(2, (1 - q)p_i + (q)g_i)/2$ to simulate 200 individuals from a population with MAFs biased toward G by q percent;
3. Perform step 2 for values of q in 0.01 increments from 0 to 1, thus generating 100 pools of 200 samples each to be classified against the F and G generated in step 1.

By creating these sets, we ensure that we have samples for which all SNPs are independent in F and G, and that F and G are samples of the same underlying population; the classification can then be observed as a function of the similarity parameter q in both cases.

2.4 Classification of real and simulated genotypes

The method as described in [1] and summarized in the Introduction was implemented using R [4]. Subsets of the real data (Sect. 2.1) and simulated data (Sect. 2.2) described above were classified in a total of 17 tests, starting with a total of 481,382 SNPs and excluding those which did not achieve a minor allele frequency >0.05 in both F and G for a given test. A summary of the tests is provided in Table 1. Additionally, a series of 200 tests using Y, f_i, and g_i as described in Sect. 2.3 were performed.

3 Results

We begin with an analytical exploration of the assumptions underlying Eq. 1,2, followed by the results of the tests as described in Methods.

3.1 D_i and T under the null hypothesis

To address the need for a fully rigorous examination of the problem which [1] tries to address, we here attempt to set up an idealized situation to which the theory and methods in [1] apply, and consider the properties of D_i and T (Eqs. 1, 2) in that setting versus deviations from that setting.

Let us assume an underlying population P with MAFs p_i from which samples F (of size n_F) and G (of size n_G) are drawn i.i.d. Consider now an additional sample Y. The null hypothesis is that Y was drawn from P, independent of F and G; the alternative of interest is that Y is drawn from G (or, symmetrically, F). Under these idealized circumstances, we observe that:

$$f_i \sim \mathsf{Bin}(2n_F, p_i)/2n_F\,, \tag{3}$$

$$g_i \sim \mathsf{Bin}(2n_G, p_i)/2n_G\,, \tag{4}$$

$$y_i \sim \mathsf{Bin}(2, p_i)/2\,, \tag{5}$$

where the factors of two are a consequence of each sample possessing two independent alleles per locus. In [1], it is proposed that T (the Z-score of D_i across all SNPs) follows a standard normal distribution (Eqs. 1,2). This proposition rests upon two assumptions: namely, that the mean $\langle D_i \rangle$ across all SNPs under the null hypothesis is zero, i.e., $\mu_0 = 0$ in Eq. 2; and that the SNPs i are completely independent such that we can write the variance of the mean as the mean variance, ie, $\mathsf{Var}(\langle D_i \rangle) = \mathsf{Var}(D_i)/s$ in the denominator of Eq. 2. Below, we consider sources of deviation from $T \sim N(0,1)$ under the null hypothesis.

3.1.1 Deviations from $\mu_0 = 0$

In the large-sample limit, under the null hypothesis,

$$\lim_{n_F\to\infty} f_i = p_i\;;\quad \lim_{n_G\to\infty} g_i = p_i\,, \tag{6}$$

and hence

$$\lim_{n_F,n_G\to\infty} D_i = \lim_{n_F,n_G\to\infty} \big(|y_i - f_i| - |y_i - g_i|\big) = 0\,. \tag{7}$$

Intuition might further suggest that since f_i and g_i are both drawn from binomial distributions which are symmetric about p_i, any sampling deviations resulting from finite n_F, n_G will fall symmetrically, and hence $\mu_0 = 0$. As we will show below, however, this conclusion is sensitive to two assumptions:

1. that the MAF differences between samples F and G, $f_i - g_i$ are small;

2. that the sample sizes n_F and n_G are not only large, but comparable.

Because the number of SNPs s is quite large, slight deviations away from $\mu_0 = 0$ have the power to shift the location of the null distribution of T considerably, rendering T incomparable to a standard normal unless the true μ_0 is known. Consider that the difference in T with and without the $\mu_0 = 0$ assumption is

$$T - T_{\mu_0=0} = \frac{\mu_0}{\sqrt{\mathsf{Var}(D_i)/s}} \tag{8}$$

and that because D_i ranges on $(-1, 1)$, $\max(\mathsf{Var}(D_i)) = 2$. This means that

$$\min(T - T_{\mu_0=0}) = \frac{\sqrt{s}}{\sqrt{2}}\mu_0 \tag{9}$$

which can be quite large for even small values of μ_0 since the number of SNPs s is on the order of 10^5. It is thus essential that μ_0 be known or controllable.

Dependence of μ_0 on slight differences in MAFs $f_i - g_i$.

Let us begin by writing the difference between MAFs f_i and g_i at locus i as τ_i,

$$f_i = g_i + \tau_i \,. \tag{10}$$

We can then write

$$D_i = |y_i - g_i - \tau_i| - |y_i - g_i| \;, \tag{11}$$

and thus

$$\mu_0 = \langle |y_i - g_i - \tau_i| - |y_i - g_i| \rangle \,, \tag{12}$$

where μ_0 is $\langle D_i \rangle$ under the null hypothesis.

We next make a simplifying assumption: since p_i are the *minor* allele frequencies and thus $0 \leq p_i \leq 0.5$, and since f_i and g_i are estimates of p_i, with few exceptions we will have $0 \leq f_i \leq 0.5$ and $0 \leq g_i \leq 0.5$ (eliminating this assumption does not significantly alter the results). Under this assumption we can write

$$|y_i - g_i - \tau_i| - |y_i - g_i| = \begin{cases} \tau_i & \text{for } y_i = 0; \\ -\tau_i & \text{for } y_i = 0.5; \\ -\tau_i & \text{for } y_i = 1. \end{cases} \tag{13}$$

and hence Eq. 12 may be written

$$\mu_0 = \sum_i \Big[\tau_i \cdot \mathbb{P}(y_i = 0|p_i) - \tau_i \cdot \mathbb{P}(y_i = 0.5|p_i) - \tau_i \cdot \mathbb{P}(y_i = 1|p_i) \Big] \; \mathbb{P}(p_i) \; \mathbb{P}(\tau_i) \,, \tag{14}$$

where $\mathbb{P}(\cdot)$ denotes probability and where we have exploited the fact that because F, G are independent samples of P, τ_i is independent of p_i, i.e., $\mathbb{P}(\tau_i|p_i) = \mathbb{P}(\tau_i)$. Observing that

$$\begin{aligned} &\mathbb{P}(y_i = 0|p_i) = (1 - p_i)^2 \,; \\ &\mathbb{P}(y_i = 0.5|p_i) = 2p_i(1 - p_i) \,; \\ &\mathbb{P}(y_i = 1|p_i) = p_i^2 \,, \end{aligned} \tag{15}$$

Eq. 14 becomes

$$\mu_0 = \sum_i \left(1 - 4p_i + 2p_i^2\right) \tau_i \, \mathbb{P}(p_i) \, \mathbb{P}(\tau_i) \tag{16}$$

$$= \langle (1 - 4p_i + 2p_i^2) \, \tau_i \rangle \, , \tag{17}$$

which is readily verified by simulation.

Eq. 17 implies that when τ_i deviates from zero, either due to systematic differences in F and G (i.e., violation of the assumption that both are drawn on the same population P) or due to sampling variation, the location of the null distribution of the test statistic given by Eq. 2 will be shifted by an amount equal to $\langle (1 - 4p_i + 2p_i^2)\tau_i \rangle \cdot \sqrt{s/\mathsf{Var}(D_i)}$ relative to that under the assumption that $\mu_0 = 0$. It is important to note that the shift is a weighted average of τ_i; ie, it depends not only on the differences in MAFs τ_i but also on p_i, and hence it is not sufficient that $\langle \tau_i \rangle = 0$, since small τ_i will be amplified when p_i is small and reduced when p_i is large. As a result, predicting the deviation away from $\mu_0 = 0$ to properly calibrate T requires knowing not only $\tau_i = f_i - g_i$, but p_i as well.

In practice, τ_i is easily calculated (examples of the distribution of τ_i for the CGEMS and HapMap CEPH groups are given in Fig. 1). On the other hand, knowing p_i requires making assumptions about the population from which Y is drawn. In the case where Y is, in fact, drawn from a different underlying population than are F and G, the p_i are difficult to obtain from the given data and the shift in T resulting from Eq. 17 is not readily calculated. (This effect is revealed in the empirical tests shown in Fig. 4, discussed in the empirical results section 3.2.1 below, wherein the HapMap samples are shifted by differing amounts.)

Dependence of μ_0 on sample sizes n_F and n_G.

The effect of deviations from the second assumption above is intuitively obvious: if $n_G > n_F$, G will better approximate the underlying population P and so will be closer on average to a future sample Y. The dependence is derived explicitly in the Appendix.

We can demonstrate this effect by simulation, as shown in Fig. 2. Here, we begin by creating 10^5 SNP MAFs p_i uniformly distributed on the interval $(0, 0.5)$. From these p_i, we simulate the g_i with sample size $n_G = 1000$ as given by Eq. 4 (i.e., a binomial sample) as well as 200 independent samples Y with y_i as given by Eq. 5. By simulating f_i per Eq. 3 as n_F is varied and computing $\langle D_i \rangle$ for each sample Y per Eq. 1, we can observe the dependence of $\langle D_i \rangle$ under the null hypothesis (i.e. μ_0) on the sample size of n_F. A plot of the result is provided in Fig. 2. As seen in the plot and derived explicitly in the Appendix, the dependence in this case varies indirectly with n_F; as expected based on the intuition above, smaller n_F leads to larger values of $\langle D_i \rangle$, indicating that Y is closer to G (the larger, more representative sample of P) than it is to F. Although the difference is small, $\langle D_i \rangle / \sqrt{\mathsf{Var}(D_i)/s}$ – given in Fig. 2(B) – is quite large, which would lead to a high false-positive rate in practice if the $\mu_0 = 0$ assumption were used and T values compared to the presumed null distribution $N(0, 1)$. Thus, we see that as n_F decreases, the distribution of T

under the null hypothesis diverges from the standard normal distribution, resulting in a higher false positive rate than that predicted by the nominal α from the standard normal.

3.1.2 Deviations from $\mathsf{Var}(\langle D_i \rangle) = \mathsf{Var}(D_i)/s$

Invocation of the central limit theorem to compare T to a standard normal distribution (as given in Eq. 2) requires that the variance of the mean of D_i be estimable by the mean of the variance, ie, $\mathsf{Var}(\langle D_i \rangle) = \mathsf{Var}(D_i)/s$. This, in turn, requires that the D_i are uncorrelated. However, if the various D_i are correlated—most notably due to linkage disequilibrium—this is no longer true. Specifically, the variance of the mean for s variables D_i with variance $\mathsf{Var}(D_i)$ and average correlation ρ amongst the distinct D_i is given by

$$\mathsf{Var}(\langle D_i \rangle) = \left(\frac{1}{s} + \frac{s-1}{s} \rho \right) \mathsf{Var}(D_i) \,. \tag{18}$$

In the case where the average correlation amongst the D_i's is zero, Eq. 18 yields the result which is found in the denominator of Eq. 2; on the other hand, $\rho \neq 0$ generates a $\big(1+(s-1)\rho\big)$ multiplicative increase over the correlationless variance. The large number of SNPs s results in little room for any correlation between them: consider that Eq. 18 dictates that for a modest number of SNPs $s = 5 \cdot 10^4$ even a very slight average correlation between all pairs of SNPs $\rho = 0.002$ would result in a tenfold increase in $\mathsf{Var}(T)$; for 500K SNPs ($s = 5 \cdot 10^5$), $\rho = 0.0002$ causes a a two order of magnitude increase in $\mathsf{Var}(T)$. However, it is impossible to ascertain ρ simply from y_i, f_i, and g_i. Instead, this issue may be addressed by choosing fewer SNPs and assuming that ρ is sufficiently small.

3.2 Results of Empirical Tests

To demonstrate the results derived in Sect. 3.1 above, as well as to explore the performance of the method in realistic situations, we carried out the computations described by Eqs. 1,2 for various F, G, and Y as described in Table 1. Distributions of T for each of the 17 tests described in Table 1 are shown in the corresponding figures listed in the table. Bearing in mind the fact that $|T| > 1.64$ yields a nominal α (p-value) of 0.05 and $|T| > 4.75$ yields a nominal $\alpha = 10^{-6}$ when compared to a standard normal distribution, the vast majority of samples we tested which were in neither F nor G were misclassified as being members of one or the other group when using the $\alpha = 0.05$ threshold for rejection of the null hypothesis; the misclassification rate was also higher than expected when using a nominal $\alpha = 10^{-6}$ threshold. The high false-positive rate in practice is attributable to sensitivity to the assumptions which underlie the method, as described above in Sect. 3.1. We present the results under the assumptions from [1] and then discuss the possibility of improving them based on our analytical and empirical findings.

3.2.1 Deviation from putative null distribution

Choice of F and G.

In Sect. 3.1.1, we saw that T will depend on the characteristics of the samples F and G. The effect is demonstrated in the results shown in Fig. 3. In these plots, T statistics (Eq. 1, 2) are given for all the CGEMS and S.1–S.5 samples for three choices of F and G:

- F = HapMap CEPH, G = CGEMS case;
- F = HapMap CEPH, G = CGEMS control;
- F = CGEMS control, G = CGEMS case.

The distribution of minor allele frequencies for each of these three groups (CGEMS cases, controls, and HapMap CEPHs) and the distribution of MAF differences for all three pairs of these groups may be seen in Fig 1. Notably, even though it may reasonably be expected that the HapMap CEPH sample closely resembles the Caucasian subjects in CGEMS, the distributions of the allele frequencies is much more similar in CGEMS cases and CGEMS controls than in either group and HapMap CEPHs. (The most striking difference in the HapMap and CGEMS distributions occurs around 0.5, where it can be seen that the minor (MAF< 0.5) allele in the CGEMS samples sometimes has a frequency > 0.5 in HapMap CEPHs.) Importantly, the width of the the distribution of MAF differences $\tau_i = f_i - g_i$ is much greater when HapMap CEPHs are one of F/G: although the mean difference in allele frequencies is quite small (0.0003–0.001) in all cases, $\mathsf{Var}(\tau_i)$ is an order of magnitude larger when HapMap CEPH is used as one of the the groups, leading to non-zero μ_0 via Eq. 17. Additionally, the sample size of the HapMap group is much smaller than that of CGEMS, thus biasing classification of an unknown sample toward the larger (and hence more representative) CGEMS sample when HapMap is used for one of the groups (cf. Sect. 3.1.1 and Appendix for associated derivations).

As expected, using the HapMap CEPHs for F fails to separate the CGEMS case and control distributions, such that CGEMS controls and cases all yield high T (and hence would all be classified as cases) when G = CGEMS cases; the situation is analogous for G = CGEMS controls (Fig. 3, top and center left). Only in the situation where F and G have similar large sample sizes and similar MAFs (when G = CGEMS cases and F = CGEMS controls) is good separation achieved, with the T statistics generally falling on the appropriate side of 0 (Fig. 3, bottom left); even so, 15 of the controls were misclassified as cases. This final case, which achieves 99.4% accuracy using $|T| > 1.64$ (nominal $\alpha = 0.05$), is analogous to the data presented in [1], for which all samples are in either F or G. As anticipated, the accuracy of the classification of cases and controls is dependent on the choice of F and G.

The classification of the 1600 samples described in Sect. 2.2 with the same choices of F and G (right column of Fig. 3) is also instructive. In all three cases, all samples achieve high T statistics despite the fact that they are in neither F nor G, frequently with $|T| \gg 4.75$, i.e., a nominal p-value less than 10^{-6}. (No simulated sample genotype was identical to any true positive genotype at greater than 62% of loci, comparable to the degree of genetic identity observed in the real samples.)

That is to say, the method classifies as positive individuals who possess a genotype y_i that is drawn on f_i or g_i, but who are not necessarily in F or G. This is unsurprising, since Eqs. 1,2 quantify the degree to which Y is not equidistant from F and G. Furthermore, this suggests that relatives of true positives may be misclassified (we consider this below in Sect. 3.2.4).

Classification of null samples when F and G are well-chosen.

Having observed the sensitivity of the classifier to the appropriate choice of F and G, we now explore the classification of samples which are in neither F nor G in the case where F and G are well-chosen. Here, we randomly select 100 cases and 100 controls from CGEMS to form an out-of-pool test sample set comprising 200 individuals, and recompute the MAFs for the remaining 1045 CGEMS cases (G) and 1042 CGEMS controls (F). (Several such random subsets were created; the results were consistent and hence we present a single representative one.) SNPs were kept subject to the same constraint (MAF>0.05 in both F and G) as above, and T statistics (Eq. 1, 2) were computed for all the test samples using f_i and g_i as described.

For the positives samples (those in F or G), the classifier performs fairly well, correctly classifying 2083 samples (and calling 4 as in neither F nor G). However, of the 200 test samples which were in neither F nor G, only 62 have $|T| < 1.64$, and the bulk are misclassified into the reduced group of CGEMS cases. The rate of false positives is thus 69% if T is used as an indicator of group membership under the assumptions in [1] at the nominal $\alpha = 0.05$ (see Table 2). A plot of the T values for all samples is given in Fig. 4(A). A similar test, in which HapMap individuals unrelated to the CGEMS participants (90 each from CEPH and YRI groups) were classified against the same subsets of 1045 CGEMS cases (G) and 1042 CGEMS controls (F), yields similar results: all the YRI individuals and 85/90 of the CEPH individuals were misclassified into the group of CGEMS cases at $\alpha = 0.05$; a plot of the T value distributions are given in Fig. 4(B). Selecting a more stringent $\alpha = 10^{-6}$ (the minimum reported in [1]) results in a 29.5% false-positive rate amongst the 200 out-of-pool CGEMS samples, 72% false-positive rate amongst HapMap CEPHs, and 100% false-positive rate amongst HapMap YRIs. A summary of the specificity and sensitivities obtained in this test is given in Table 2.

The reason for the high false-positive rates in practice despite the stringent nominal false positive rate is clear from the plots Fig. 4(A,B): namely, it can be seen that the putative null distribution (light grey line, $N(0,1)$, cf Eq. 2) does not correspond to the observed distribution for samples for which the null hypothesis is correct, with differences in both the location and width.

The overall shift to the right is a product of the small differences in $f_i - g_i$ which accumulate as given by Eq. 17. Because in this test we happen to know the MAFs p_i along with f_i and g_i for each of the CGEMS samples, we can compute μ_0 given by Eq. 17 as $1.133 \cdot 10^{-4}$ and verify that, when divided by the average $\sqrt{\mathsf{Var}(D_i)/s} \approx 5.6 \cdot 10^{-5}$ amongst the samples, the center of the observed null distribution will be at $T \approx 2$. Indeed, visual inspection of Fig. 4(A) shows that shifting each T distribution by -2 would result in F, G, and null-sample distributions which lie more symmetrically about $T = 0$. Note, also, that the HapMap CEPHs and YRIs are shifted by different amounts than

are the CGEMS samples, due to the fact that the p_i's which underlie the HapMap samples differ from each other and from CGEMS. From this, we can see that samples Y which are not drawn on the same population as F and G may in practice have a high false positive rate.

The effect of LD, derived in Sect. 3.1.2, is also seen in these examples. In Fig. 4(B), we observe a narrower distribution of T for the HapMap YRI samples versus the Caucasian CGEMS participants and HapMap CEPHs (the Yoruban individuals, who come from an older population, have lower average LD). The same effect is observed by comparing the distribution of T for the simulated samples in Fig. 3 (for which each SNP was independently sampled and hence have artificially low LD) to those of real populations.

3.2.2 Correcting for deviations from $N(0,1)$

Although the empirical false-positive rates obtained the the tests described above are exceedingly high, the distributions of T obtained in Fig. 4(A,B) are nonoverlapping. Hence, one might expect that if one could appropriately calibrate the thresholds of T at which classification is made, the sensitivity and specificity of the test could be considerably improved. (Note that, in practice, one does not know where the true-positive F and G distributions of T lie; this requires the genotypes of the F and G individuals.) Two approaches may be taken toward calibrating classification thresholds for T: an analytical approach, based on the results in Sect. 3.1 above; or an empirical approach, based on constructing a null distribution from available samples. As we will see, both these approaches pose substantial difficulties.

Analytical approach.

In order to correct for the deviations from $N(0,1)$ analytically, we need to know both the location and width of the distribution of T in the non-ideal circumstances under which the test is being conducted. That is, we need to know deviations from $\mu_0 = 0$ resulting from MAF differences $f_i - g_i$ and sample size differences of n_F and n_G (cf. Sect. 3.1.1 and Appendix), as well as the average correlation amongst SNPs ρ (cf. Sect. 3.1.2, Eq. 18).

Let us first consider the result in Eq. 17, which shows that μ_0 in practice will be a function of the MAF differences $\tau_i = f_i - g_i$ as well as the MAFs p_i of the population P of which Y is a sample. If we are well-assured that F and G are large samples of the same population P and that Y is also a sample of that population, an average of f_i and g_i may be used to estimate p_i (the y_i, while necessarily drawn on p_i, are too small a sample to be a good estimate) and thus obtain μ_0. Results of this approach (for the tests shown in Fig. 4 and Table 2) are given in Table 3, in which p_i was estimated as $(n_G \cdot g_i + n_F \cdot f_i)/(n_G + n_F)$ and μ_0 was computed according to Eq. 17. A slight improvement in the performance of the method can be seen by comparing the first two columns of Table 2 to those of Table 3.

However, the assumption used to compute p_i (i.e., that Y, F, and G are all i.i.d. samples of the same population P) is one on which the accuracy of the correction is strongly dependent; consider, for instance, that the $\mu_0 \approx 1.133 \cdot 10^{-4}$ obtained for the simulations in Fig. 4(A,B) and discussed

above will produce the appropriate shift $T \approx T_{\mu_0=0} - 2$ for the 200 CGEMS samples in Fig. 4(A) using this method, but will not centralize the HapMap T distributions in Fig. 4(B) appropriately, because the f_i and g_i are not good estimates of the MAFs of the populations from which the HapMap samples are drawn. Applying this correction to the HapMap samples (equivalent to moving the HapMap T distribution two units to the left in Fig. 4(B)) results in a misclassification rate of 86% (nominal $\alpha = 0.05$) and 44% (nominal $\alpha = 10^{-6}$) for the HapMap CEPHs and continued 100% misclassification of all HapMap YRIs. It is thus essential that if the μ_0 given by Eq. 17 is to be used, sound estimates of p_i need to be obtained. When Y is not a sample of the same population as F or G, estimates of p_i are unobtainable from f_i, g_i and y_i alone, and hence this correction relies upon the assumption that G, F, and Y are well-matched.

The second influence on μ_0, described in both Sect. 3.1.1 and the Appendix, is the effect of the sample sizes n_F and n_G. Here, corrections are readily made, provided the sample sizes of F and G are known. In a forensics context, where G is a sample of unknown composition, n_G may not be known; on the other hand, in other contexts (such as when using case and control MAFs from a GWAS), sample sizes are known and readily adjusted for. (In this test, $n_F \approx n_G \approx 1000$, and the correction is negligible.)

We also saw in Sect. 3.1.2 and Fig. 4(B) that the distribution of T for null samples will depend on the degree of correlation between the SNPs. To accurately derive the width of the T distribution for null samples, one would need to either select SNPs that yield vanishingly small ρ or know the value of ρ with high accuracy for the population of which Y is a sample so that it can be discounted. The latter option requires knowledge beyond the MAFs of F and G and the genotype of individual Y; namely, it requires multiple genotypes from the population P from which Y was drawn such that the average correlation ρ between SNPs can be computed; even with a collection of null genotypes, the computation of the average pairwise correlation for 10^5 SNPs is a computationally unfeasible task. Rather, selecting fewer SNPs in order to reduce LD is a more workable solution; the results of this approach can be seen in Fig. 4(C,D) and in Table 2. Here, 50,000 SNPs were selected, uniformly distributed across of the $481,382$ SNPs used in Fig. 4(A,B). 50,000 SNPs was shown in [1] to be a reasonable lower bound to detect at nominal $\alpha \approx 10^{-5}$ one individual amongst 1000, which is the concentration of true positive individuals in this test.

As is clear from Fig. 4, reducing the number of SNPs narrows the distributions considerably, yet at the same time brings them closer together such that the crisp separation previously obtained is reduced. Using this method, we see that the 200 CGEMS samples now have a distribution closer to that of the putative null $N(0,1)$ such that using a threshold of $\alpha = 0.05$ yields an improved—yet still larger than nominal—21% false-positive rate while maintaining a high 96.3% true positive rate. However, the misclassification rate is still over 50% for both HapMap samples, and improving these values requires compromising the sensitivity, a direct result of the overlapping T distributions for the G and HapMap samples.

Finally, we can consider applying both the SNP reduction and the μ_0 correction applied above;

the results here are given in the final two columns of Table 3. Because F and G are well-matched and the μ_0 correction given by Eq. 17 is slight in the case of these 50,000 SNPs, the correction happens to offer little improvement over that achieved by subsetting the SNPs.

Empirical approach.

Another potential approach to obtaining a correct null distribution is purely empirical, namely, collecting a set of presumed-null genotypes (called N) which can be assumed to be drawn from the same population as Y, and determining the distribution of T for the null samples N. However, once again the method's sensitivity to the assumptions are a source of error.

To see this, let us once more return to Fig. 4. In these figures, vertical bars represent the 0.05 and 0.95 quantiles of the 200 CGEMS (black), 90 HapMap CEPH (cyan) and 90 HapMap YRI (blue) T distributions.

Let us first consider a situation in which we have f_i and g_i, along with an individual Y who is one of the 200 CGEMS samples not in F or G, but no other genotypes. We might reasonably turn to publicly available HapMap genotypes as our group N from which we construct an empirical null distribution from which we set thresholds. The lines in Fig. 4(A,C) depict this case. Using thresholds obtained from the HapMap CEPH distribution (cyan lines) still incorrectly classifies half of the 200 CGEMS samples; the false positive rate is yet greater (and the true-positive rate smaller) when using the HapMap YRI distribution. These lines illustrate the importance of choosing for N a sample which closely resembles Y—as with the choice of F for a given G in Sect. 3.2.1, HapMap CEPHs are insufficiently similar to CGEMS to provide accurate results, despite the fact that both samples are Americans of European descent.

The converse is true as well: if we have N, F, and G which are well matched—such as illustrated in Fig. 4(B,D), in which N, F, and G all come from CGEMS data—yet Y is not drawn from the same underlying population as $N/F/G$, the method will incorrectly classify Y; roughly a quarter of the HapMap CEPHs and the majority of HapMap YRIs lie outside the thresholds set by the 200 CGEMS samples in Fig. 4(B,D). Once again, this underscores the importance of the assumption that F, G, and Y are all i.i.d. samples of the same population P, and—if a sample N is being used to construct a null distribution empirically—it, too, must be an i.i.d. sample of P.

Another empirical option is that of simulating genotypes from the f_i and g_i to simulate T under the *alternative* hypothesis, with the assumption that the null and alternative hypothesis T distributions do not strongly overlap. However, this method also requires that F and G are large and well-matched samples, since (as can be seen in the top- and middle-right graphs in Fig. 3) poorly-matched F and G will not produce crisply separated distributions. Furthermore, the thresholds derived by this approach will relate not to the false-positive rate but rather to the false-negative rate, i.e., these thresholds would control the power of the test, and the specificity in practice will remain unknown.

We have thus seen that small deviations from the assumptions that F, G, and Y are i.i.d. samples of the same population P can produce false-positive rates which greatly exceed those

predicted by the null hypothesis. Even when these sources of error were adjusted for, in our tests we still observed a false positive rate that was higher than expected, such that the false positive rate was never less than 20% in practice for a nominal false-positive rate of 5%, and never less than 13% at a nominal false-positive rate of 0.0001%. While the distributions of T for the F, G, and various Y samples were observed to be separate in Fig. 4, we find that calibrating the thresholds accurately in absence of genotype information for F and G is not obviously doable. More importantly, it is not clear that, once thresholds are chosen, the empirical specificity could be assessed without additional genotype information from subjects who are well-matched to F, G and Y.

3.2.3 Positive predictive value of the method.

The effect of the modest specificity—even in the best of cases described above—on the posterior probability that the individual Y is in F or G is considerable, given that the prior probability is likely to be relatively small in most applications of this method. Let us consider the positive predictive value (PPV), which quantifies the post-test probability that an individual Y with a positive result (i.e., significant T) is in F or G. This probability depends on the prior probability that the individual is in F or G, i.e., on the prevalence of being a member of F or G. PPV follows directly from Bayes' theorem, and is defined as

$$\mathsf{PPV} = \frac{\mathsf{Sens} \cdot \mathsf{Prev}}{\mathsf{Sens} \cdot \mathsf{Prev} + (1 - \mathsf{Spec})(1 - \mathsf{Prev})}\,, \tag{19}$$

where the PPV is the posterior probability that Y is in F/G given a prior probability of Prev. We can write this equivalently in terms of the positive likelihood ratio LR_+,

$$\mathsf{Posterior\,odds} = \mathsf{LR}_+ \cdot \mathsf{Prior\,odds} \tag{20}$$

$$\mathsf{LR}_+ = \frac{\mathsf{Sens}}{(1 - \mathsf{Spec})}\,. \tag{21}$$

A plot of PPV vs. prevalence is given in Fig. 5. Even with the best sensitivity (99.23%) and specificity (87%) obtained in our tests—that in which F, G, and Y were drawn on the same underlying population P, μ_0 was accurately computed, and a nominal $\alpha = 10^{-6}$ was used as a threshold (cf. Table 3)—the prior probability (prevalence) of Y being in F/G needs to exceed 54% in order to achieve a 90% post-test probability that the subject is in F/G. For a PPV of 99%, the prior probability needs to exceed 72% for any specificity under 95%, assuming the observed sensitivity of 99%. We thus see the strong need for prior belief that Y is in F or G.

The difficulty in assessing the (empirical) specificity of the test in absence of additional data makes the posterior probability difficult to ascertain since the false positive rate in practice is much greater than that given by the nominal false-positive rate α. Eq. 21 underscores this fact; referring once more to the best result in Tables 2, 3, consider that LR_+ at 87% specificity and 99% sensitivity is 7.6, versus 990000 if the nominal false-positive rate $\alpha = 10^{-6}$ were correct. For prior probability of 1/1000, the first case yields a posterior probability of 1.1/1000, while the second

yields a posterior probability of 998/1000. These differences, which are difficult to measure without additional, well-matched null sample genotypes and which depend strongly on the degree to which the assumptions underlying the method are met (consider the differences between the CGEMS and HapMap CEPH specificities in Tables 2, 3), pose a severe limitation on the utility of using Eqs. 1,2 to resolve Y's membership in samples F or G.

3.2.4 Classification of relatives

We now turn to the classification of individuals who are relatives of true positives. As discussed above in Sect. 3.2.1, the results from simulations S.1–S.5 in Fig. 3 suggest that individuals who are genetically similar, but not identical to, the subjects in pools F and G, frequently exhibit high $|T|$. This effect can be investigated by using HapMap families, since we can reasonably expect that the children will bear a greater resemblance to their parents than their parents do to one another. Recalling that the HapMap pools consist of thirty individual mother-father-offspring pedigrees, we construct pools as follows:

- F = Mothers from pedigrees 1–15 and fathers from pedigrees 1–15
- G = Children from pedigrees 1–15 and fathers from pedigrees 16–30

and then compute T for mothers and children from pedigrees 16–30 using the same SNP criteria as before. The results of these tests for both the CEPH and YRI pedigrees, given in Fig. 6, are as expected, with the children having a significantly higher distribution of T than the mothers; the T values for all the children were so large that p-values $\ll 10^{-16}$ were obtained when comparing to $N(0,1)$. By contrast, 5/15 of the YRI mothers from pedigrees 16–30 and 10/15 of the CEPH mothers from pedigrees 16–30 yielded $|T| > 1.64$ (with distributions roughly centered about $T = 0$). The wider distribution amongst the CEPHS again reflects the effect of LD. In Fig. 6 we can see that the method has the power to resolve three groups: those in a group, those related to members of a group, and those who are neither (as the groups become bigger, and hence more homogeneous, we would expect the distributions to move closer together, as evidenced by the lower range of T for the CGEMS-based tests in Fig. 3). Note, however, that without knowing the distribution of T for true positives (which necessitates knowing the genotypes of true positives) setting a threshold to distinguish between true positives and their relatives is not possible by any of the methods described above.

In order to explore the effect of genetic similarity in a controlled, ideal situation for which F and G are known to be samples of the same underlying population and for which all SNPs are known to be independent (i.e., in the ideal situation in which the putative null distribution $N(0,1)$ should hold), we carried out the simulations described in Sect. 2.3. In these simulations, the underlying population P was taken to have MAFs p_i as given by the CGEMS controls; f_i, g_i, and y_i were derived as described in Sect. 2.3 as binomial samples of p_i.

In the first of these simulations, the test samples were constrained to have a proportion q of SNPs identical to a true positive individual, with the remaining SNPs drawn on p_i. A plot of the false positive rate, defined as the fraction of the 200 simulated samples that achieve significant $|T| > 1.64$ ($\alpha < 0.05$), as the similarity parameter q is varied is shown in Fig. 7. Once simulated samples exceeded 65% identity with a true positive individual, they universally achieve significant T, and significant values of T are found over half the time for simulated samples exceeding 60% identity. (It should be noted that of the real samples, no two had $> 62\%$ fractional identity.)

In the second set of these simulations, the test samples were drawn from a weighted mixture of MAFs:

$$y_i \sim \mathsf{Bin}(2, p'_i)/2\,, \tag{22}$$

$$p'_i = (1-q)p_i + (q)g_i\,, \tag{23}$$

i.e., the sample was drawn from MAFs p'_i which are q percent like G and $(1-q)$ like CGEMS controls (MAFs p_i). By simulating 200 samples for various q, computing T for each sample using the simulated F and G, and counting the number of samples that achieve significant $|T| > 1.64$ at $\alpha = 0.05$, we can see how the false positive rate varies with the percentage of G. Results are given in Fig 7. The misclassification rate exceeds 50% for $q = 0.05$; at $q = 0.1$, all samples yield significant T.

The misclassification of relatives follows directly from the method's premise. Eqs. 1,2 together answer whether *individual's genotype y_i is closer to sample G's MAFs g_i than to sample F's MAFs f_i than would be expected by chance*, and it is unsurprising that a relative of a true member of G would appear closer to G (via Eqs. 1,2) than to F.

Put another way, Y being a member of G is *sufficient* but not *necessary* for y_i to be closer (via Eq. 1) to g_i than to f_i; it is possible for other sources of genetic variation to cause y_i to be closer g_i than to f_i. We can observe this by turning once again to Fig. 4(A,C), where the dashed red and green lines show that the not-in-G CGEMS cases had a distribution of T closer to the other CGEMS cases G, and the not-in-F CGEMS controls had a distribution of T closer to the other CGEMS controls F, indicating that small class-specific genetic differences can yield altered values of T. The erroneous inferential leap that significant T results from Y's presence in F or G is responsible for the misclassification of relatives as well as for misclassification of non-relatives in the previous examples.

4 Discussion and Conclusions

In this work, we have further characterized and tested the genetic distance metric initially proposed in [1]. This metric, summarized here by Eqs. 1,2, quantifies the distance of an individual genotype Y with respect to two samples F and G using the marginal minor allele frequencies f_i and g_i of the two samples and the genotype y_i. The article [1] proposes to use this metric to infer the

presence of the individual in one of the two samples, and the authors demonstrate the utility of their classifier on known positive samples (i.e., samples which are in either F or G) showing that in this situation their method yields classifications of high sensitivity. Our investigations reveal that while the sensitivity is quite high (correctly classifying true positives into groups F and G) the specificity is considerably less than that predicted by the quantiles of the putative null distribution $N(0,1)$. As a result, Eqs. 1, 2 are severely limited in their utility for discerning Y's presence in samples F or G.

In this work we have shown that high T values, significant when compared against $N(0,1)$, may be obtained for samples that are in neither of the pools tested under several circumstances:

- when pools F and G are sufficiently dissimilar such that the differences in f_i and g_i dominate, as seen in Sects. 3.1.1 and 3.2.1 as well as the Appendix;
- when Y is a sample of a different population than are F and G, as seen in Sect. 3.2.1;
- when a small amount of average LD is present such that the putative null distribution in Eq. 2 does not hold (due to a violation of the CLT assumption of independence), as seen in Sects. 3.1.2 and 3.2.1;
- and when a sample is genetically similar, but not identical to, individuals comprising F or G (e.g., relatives of true positives), as seen in Sect. 3.2.4.

The high false positive rates in the first two cases result from assumptions underlying the putative null distribution which are not met in practice, specifically, that the individual Y along with samples F and G are all i.i.d. samples of the same underlying population P, and that the amount of correlation between all s SNPs is vanishingly small. As we saw in Sect. 3.2.1 and 3.2.2, these assumptions are difficult to meet; for instance, HapMap CEPH and CGEMS samples are sufficiently dissimilar that they introduce error in violation of the first assumption, despite the fact that both samples are Americans of European descent. Adjusting for deviations from the putative null distribution also requires making strong assumptions or obtaining additional information, as seen in Sect. 3.2.2.

Additionally, the conclusion that high T values result from Y's presence in G relies upon the questionable assumption that individuals in neither F nor G will be equidistant from both, resulting in false positives even when the other assumptions are met. For instance, similarly genotyped individuals (both relatives and simulated samples) are often classified into the same group despite the fact that the other assumptions were met (Sect. **??**). Amongst non-relatives, even when the thresholds have been adjusted for violations of the above assumptions as in Sect. 3.2.2, Eqs. 1,2 produce misleading classifications at a rate that is considerably greater than expected (21% vs. nominal 5% and 13% vs. nominal 0.0001% in the best cases reported in Table 2). The unpredictable false positive rate in practice, resulting from the difficulty in accurately calibrating the significance of T, results in a likelihood ratio (and hence post-test probability) that is also unpredictable, with

higher false positive rates yielding lower post-test probabilities. When the prior probability of Y's presence in F or G is modest, strong evidence (i.e., high specificity) is needed to outweigh this prior, which was not achieved in our tests (Sect 3.2.4). On the other hand, when samples were known *a priori* to be in one of the groups F/G, Eqs. 1,2 correctly identify the sample of which the individual is part (Sect. 3.2.4).

These findings have implications both in forensics (for which the method [1] was proposed) and GWAS privacy (which has become a topic of considerable interest in light of [1]). We briefly consider each:

Forensics implications.

The stated purpose of the method—namely, to positively identify the presence of a particular individual in a mixed pool of genetic data of unknown size and composition—is difficult to achieve. In this scenario, we have g_i (from forensic evidence) and a suspect genotype y_i. To apply the method, we would need 1) to assume that Y and G are indeed i.i.d. samples of the same population P; 2) to obtain a sample F which is *also* a sample of the underlying population P, well-matched in size and composition to G; 3) to obtain an estimate of the sample size of G such that sample-size effects can be appropriately discounted; and 4) to assume that the p-values at the selected classification thresholds are accurate. We have seen in the Results section the sensitivity to the assumption that Y, F, and G all come from the same population, the sensitivity to the sample size of G, and the difficulties in calibrating thresholds; the high false-positive rates which result from even small violations of these assumptions make it exceedingly likely that an innocent party will be wrongly identified as suspicious; its is even more likely for a relative of an individual whose DNA is present in G.

GWAS privacy implications.

Here the scenario of concern is that of a malefactor with the genotype of one (or many) individuals, and access to the case and control MAFs from published studies; could the malefactor use this method to discern whether one of the genotypes in his possession belongs to a GWAS subject? In this case, F and G are known to be samples of the same underlying population P (due to the careful matching in GWAS), and their sample sizes are large and known. However, the malefactor still needs 1) to assure that Y is a member of this population as well (as shown by the poor results when HapMap samples were classified using CGEMS MAFs) and 2) to assume that the p-values at the selected classification thresholds are accurate. Additionally, the prior probability that any of the genotypes in the malefactor's possession comes from a GWAS subject is likely to be quite small, since GWAS samples are a tiny fraction of the population from which they are drawn. Even if the malefactor were able to narrow down the prior probability to one in three, a sensitivity of 99% and a specificity of 95% is needed to obtain a 90% posterior probability that the individual is truly a participant.

On the other hand, if the malefactor *does* have prior knowledge that the individual Y partic-

ipated in a certain GWAS but does not know Y's case status, Eqs. 1, 2 permit the malefactor to discover with high accuracy which group Y was in. Additionally, in the case of *a priori* knowledge, the participant's genotype is not strictly necessary, since a relative's DNA will yield a large T score that falls on the appropriate F/G side of null.

Despite these limitations, we have found that the distance metric (Eqs. 1, 2) may still have forensic and research utility. It is clear from both our studies and the original paper [1] that the sensitivity is quite high; in the (rare) case that a sample has an insignificant $|T| < 1.64$, it is very likely that Y is in neither F nor G. We can also see that genetically distinct groups have T distributions with little overlap (Fig. 4), and so it may be worth investigating the utility of Eqs. 1,2 for ancestry inference.

On this note, let us once more consider the quantity which Eq. 1 measures, namely the distance of y_i from f_i relative to the distance of y_i from g_i. Referring to Fig. 3 (right column) and Fig. 4(A,C), we can see that samples Y which are more like those in sample G have a distribution that lies to the right of samples which are more similar to F, as expected; for example, in Fig. 4(A,C), the distribution of null (not in F, G) CGEMS cases (dashed red line) is shifted to the right with respect to the distribution of null CGEMS controls, as might be expected from Eq. 1, i.e., the CGEMS case Ys are closer to CGEMS case Gs than are the CGEMS control Ys. Although this difference is not statistically significant, one could imagine that it may be possible to select SNPs for which the shift is significant, i.e., a selection of SNPs for which unknown cases are statistically more likely to be closer (via Eq. 1) to the cases in G and unknown controls are statistically more likely to be closer to the controls in F. In this case, a subset of SNPs known to be associated with disease may potentially be used with Eqs. 1, 2 to predict the case status of new individuals; conversely, finding a subset of SNPs which produce significant separations of the test samples may be indicative of a group of SNPs which play a role in disease. Because this type of application would use fewer SNPs and would involve the comparison of two distributions of T (cases $\notin \{F, G\}$ vs. controls $\notin \{F, G\}$), it may be possible to circumvent some of the problems stemming from the unknown width and location of the null distribution described above; still, much work is needed to investigate this possible application. If successful, the metric proposed in [1], while failing to function as a tool to positively identify the presence of a specific individual's DNA in a finite genetic sample, may if refined be a useful tool in the analysis of GWAS data.

Appendix: Dependence of μ_0 on the sample size of F and G

Consider $\langle D_i \rangle$ (cf. Eq. 1) under the null hypothesis assumptions that Y, F, and G are all drawn i.i.d. from the same underlying population P with MAFs p_i. Writing the probability distribution

of p_i as $\mathbb{P}(p_i)$, $\langle D_i \rangle$ is given by

$$\langle D_i \rangle = \langle |y_i - f_i| - |y_i - g_i| \rangle = \langle |y_i - f_i| \rangle - \langle |y_i - g_i| \rangle \tag{A-1}$$

$$\begin{aligned} &= \iiint_{-\infty}^{\infty} |y_i - f_i| \;\; \mathbb{P}(y_i|p_i)\, \mathbb{P}(f_i|p_i)\, \mathbb{P}(p_i)\, dy_i\, df_i\, dp_i - \\ &\qquad - \iiint_{-\infty}^{\infty} |y_i - g_i| \;\; \mathbb{P}(y_i|p_i)\, \mathbb{P}(g_i|p_i)\, \mathbb{P}(p_i)\, dy_i\, dg_i\, dp_i \;, \end{aligned} \tag{A-2}$$

where we exploit the fact that Y, F and G are independent of each other but depend on the underlying population MAFs.

The dependence of the first (second) term in Eq. A-2 on n_F (n_G) is derived as follows. First, we note that since each y_i is two Bernoulli trials (two alleles) with probability p_i, we have the following values of $|y_i - f_i|$ with probability $\mathbb{P}(y_i|p_i)$ for each allowable value of y_i:

$$|y_i - f_i| \cdot \mathbb{P}(y_i|p_i) = \begin{cases} \big(1 - f_i\big) \cdot \big(p_i^2\big) & \text{for } y_i = 1\,; \\ \big(\,|0.5 - f_i|\,\big) \cdot \big(2p_i(1-p_i)\big) & \text{for } y_i = 0.5\,; \\ \big(f_i\big) \cdot \big((1-p_i)^2\big) & \text{for } y_i = 0\,. \end{cases} \tag{A-3}$$

Moreover, since each f_i follows a binomial distribution of size $2n_F$ (two alleles per person), we invoke the normal approximation to the binomial for values of $n_F > 10$ with mean p_i and variance $p_i(1-p_i)/(2n_F)$. Hence:

$$\mathbb{P}(f_i|p_i) \;\; = \;\; \sqrt{\frac{2n_F}{2\pi p_i(1-p_i)}}\, \exp\left[-\frac{2n_F(f_i - p_i)^2}{2p_i(1-p_i)}\right] \tag{A-4}$$

$$\;\; = \;\; \frac{A_{F,i}}{\sqrt{\pi}} \exp\left[-A_{F,i}^2 (f_i - p_i)^2\right], \tag{A-5}$$

where we introduce

$$A_{F,i} = \sqrt{n_F/(p_i(1-p_i))} \tag{A-6}$$

to simplify the notation. In consequence, the first term of Eq. A-2 can be written:

$$\iint_{-\infty}^{\infty} \Big[(1-f_i)(p_i^2) + (|0.5 - f_i|)(2p_i(1-p_i)) + (f_i)((1-p_i)^2)\Big] \cdot \\ \cdot \frac{A_{F,i}}{\sqrt{\pi}} \exp\Big[-A_{F,i}^2 (f_i - p_i)^2\Big] \mathbb{P}(p_i)\, df_i\, dp_i \tag{A-7}$$

and the second term may be written analogously for G. The absolute value in Eq. A-7 is dealt with by considering the $f_i \geq 0.5$ and $f_i \leq 0.5$ cases separately, i.e., treating Eq. A-7 as the sum of integrals

$$\int_{-\infty}^{\infty} \left[\int_{0.5}^{\infty} \Big((1-f_i)(p_i^2) + (f_i - 0.5)(2p_i(1-p_i)) + (f_i)((1-p_i)^2) \Big) \mathbb{P}(f_i|p_i)\, df_i + \right. \\ \left. + \int_{-\infty}^{0.5} \Big((1-f_i)(p_i^2) + (0.5 - f_i)(2p_i(1-p_i)) + (f_i)((1-p_i)^2) \Big) \mathbb{P}(f_i|p_i)\, df_i \right] \mathbb{P}(p_i)\, dp_i \tag{A-8}$$

Expanding the polynomials in Eq. A-8 and once more using Eq. A-6 to simplify notation, we rewrite the above as

$$\int_{-\infty}^{\infty} \frac{A_{F,i}}{\sqrt{\pi}} \left[\int_{0.5}^{\infty} \big(C_1 f_i + C_2\big) e^{-A_{F,i}^2 (f_i - p_i)^2} df_i + \right. \\ \left. + \int_{-\infty}^{0.5} \big(C_3 f_i + C_4\big) e^{-A_{F,i}^2 (f_i - p_i)^2} df_i \right] \mathbb{P}(p_i)\, dp_i \quad \text{(A-9)}$$

where C_1, C_2, C_3, and C_4 are functions of p_i but independent of f_i:

$$C_1 = 1 - 2p_i^2\,, \quad \text{(A-10)}$$

$$C_2 = 2p_i^2 - p_i\,, \quad \text{(A-11)}$$

$$C_3 = 1 - 4p_i + 2p_i^2\,, \quad \text{(A-12)}$$

$$C_4 = p_i\,. \quad \text{(A-13)}$$

Performing the interior integration in Eq. A-9 yields

$$\int_{-\infty}^{\infty} \frac{A_{F,i}}{\sqrt{\pi}} \left[(C_1 - C_3) \left(\frac{e^{-A_{F,i}^2 (0.5 - p_i)^2}}{2A_{F,i}^2} \right) + (C_3 p_i + C_4) \left(\frac{\sqrt{\pi}}{A_{F,i}} \right) + \right. \\ \left. + \Big((C_1 - C_3) p_i + (C_2 - C_4) \Big) \left(\frac{\sqrt{\pi}\, \mathrm{erfc}\big(A_{F,i}(0.5 - p_i)\big)}{2A_{F,i}} \right) \right] \mathbb{P}(p_i)\, dp_i\,. \quad \text{(A-14)}$$

Expanding out the various Cs as well as $A_{F,i}$, we now have for the first term of $\langle D_i \rangle$

$$\int_{-\infty}^{\infty} \big(p_i(1-p_i)\big) \left[2\sqrt{\frac{p_i(1-p_i)}{\pi\, n_F}} \exp\left(-\frac{n_F (0.5 - p_i)^2}{p_i(1-p_i)} \right) + \right. \\ \left. + 2(1-p_i) + (2p_i - 1)\mathrm{erfc}\left(\sqrt{\frac{n_F (0.5 - p_i)^2}{p_i(1-p_i)}} \right) \right] \mathbb{P}(p_i)\, dp_i\,, \quad \text{(A-15)}$$

which has an indirect dependence on n_F. Performing the same integration for the second term in Eq. A-2 yields analogous indirect n_G dependence. As a result, when $n_F < n_G$, the first term is greater than the second, yielding $\langle D_i \rangle > 0$; in the limit $n_F, n_G \to \infty$, this difference becomes smaller.

The dependence is illustrated in Fig. 2A. Here, we assume a uniform distribution of p_i on $(0, 0.5)$ and construct 10^5 p_i's for the underlying population P from which we draw, independently, a sample G of size $n_G = 1000$ and 200 samples Y from which we estimate $\langle D_i \rangle$ under the null hypothesis. Sample F is drawn i.i.d. from P with sample sizes ranging from $n_F = 10$ to $n_F = 1000$, permitting us to plot $\langle D_i \rangle$ as n_F is varied. The simulation results are shown as circles, overlayed with a plot of Eq. A-2 using the result in Eq. A-15 and assuming the uniform distribution of p_i. The values for $\langle D_i \rangle$ obtained from the simulation closely matches those derived from Eq. A-15. In Fig. 2B, the corresponding values of T are presented.

Acknowledgments

This research was supported by the Intramural Research Program of the National Cancer Institute, National Institutes of Health, Bethesda, MD. RB was supported by the Cancer Prevention Fellowship Program, National Cancer Institute, National Institutes of Health, Bethesda, MD.

References

[1] Nils Homer, Szabolcs Szelinger, Margot Redman, David Duggan, Waibhav Tembe, Jill Muehling, John V Pearson, Dietrich A Stephan, Stanley F Nelson, and David W Craig. Resolving individuals contributing trace amounts of DNA to highly complex mixtures using high-density SNP genotyping microarrays. *PLoS Genetics*, 4(8):e1000167, 2008.

[2] David J Hunter, Peter Kraft, Kevin B Jacobs, David G Cox, Meredith Yeager, Susan E Hankinson, Sholom Wacholder, Zhaoming Wang, Robert Welch, Amy Hutchinson, Junwen Wang, Kai Yu, Nilanjan Chatterjee, Nick Orr, Walter C Willett, Graham A Colditz, Regina G Ziegler, Christine D Berg, Saundra S Buys, Catherine A McCarty, Heather Spencer Feigelson, Eugenia E Calle, Michael J Thun, Richard B Hayes, Margaret Tucker, Daniela S Gerhard, Joseph F Fraumeni, Robert N Hoover, Gilles Thomas, and Stephen J Chanock. A genome-wide association study identifies alleles in FGFR2 associated with risk of sporadic postmenopausal breast cancer. *Nature Genetics*, 39(7):870–874.

[3] The International HapMap Consortium. The International HapMap Project. *Nature*, 426(6968):789–796.

[4] R Development Core Team. *A language and environment for statistical computing.* Vienna, Austria, 2004.

Y individuals	F population	G population	T distribution
1145 CGEMS cases 1142 CGEMS controls S.1 – S.5	60 unrelated HapMap CEPH	1145 CGEMS cases	Fig. 3
1145 CGEMS cases 1142 CGEMS controls S.1 – S.5	60 unrelated HapMap CEPH	1142 CGEMS controls	Fig. 3
1145 CGEMS cases 1142 CGEMS controls S.1 – S.5	1142 CGEMS controls	1145 CGEMS cases	Fig. 3
100 CGEMS cases not in G 100 CGEMS controls not in F 90 HapMap CEPH 90 HapMap YRI	1042 CGEMS controls	1045 CGEMS cases	Fig. 4
HapMap YRI mothers 16–30 HapMap YRI children 16–30	HapMap YRI mothers 1–15 and fathers 1–15	HapMap YRI children 1–15 and fathers 16–30	Fig. 6
HapMap CEPH mothers 16–30 HapMap CEPH children 16–30	HapMap CEPH mothers 1–15 and fathers 1–15	HapMap CEPH children 1–15 and fathers 16–30	Fig. 6

Table 1: Summary of tests performed. In the last four rows, the numbers refer to the families in the HapMap YRI and CEPH populations, such that child 1 is the offspring of mother 1 and father 1, et cetera.

	481,382 SNPs		50,000 SNPs	
	$\alpha = 0.05$	$\alpha = 10^{-6}$	$\alpha = 0.05$	$\alpha = 10^{-6}$
Sensitivity	99.8%	97.5%	96.3%	36.3%
Specificity, 200 CGEMS	31.0%	70.5%	79.0%	99.5%
Specificity, 90 HapMap CEPH	5.5%	27.7%	45.5%	100.0%
Specificity, 90 HapMap YRI	0.0%	0.0%	4.4%	97.7%

Table 2: Empirical sensitivity and specificity for the tests shown in Fig. 4 assuming $\mu_0 = 0$. Classification results are given for two different nominal false positive rates $\alpha = 0.05$ and $\alpha = 10^{-6}$.

	481,382 SNPs		50,000 SNPs	
	$\alpha = 0.05$	$\alpha = 10^{-6}$	$\alpha = 0.05$	$\alpha = 10^{-6}$
Sensitivity	99.90%	99.23%	97.36%	31.09%
Specificity, 200 CGEMS	40.0%	87.0%	78.0%	99.5%
Specificity, 90 HapMap CEPH	14.4%	55.5%	54.4%	100.0%
Specificity, 90 HapMap YRI	0.0%	0.0%	7.7%	100.0%

Table 3: Empirical sensitivity and specificity for the tests shown in Fig. 4 using μ_0 as given by Eq. 17 and assuming that $p_i = (n_F \cdot f_i + n_G \cdot g_i)/(n_F + n_G)$. Classification results are given for two different nominal false positive rates $\alpha = 0.05$ and $\alpha = 10^{-6}$.

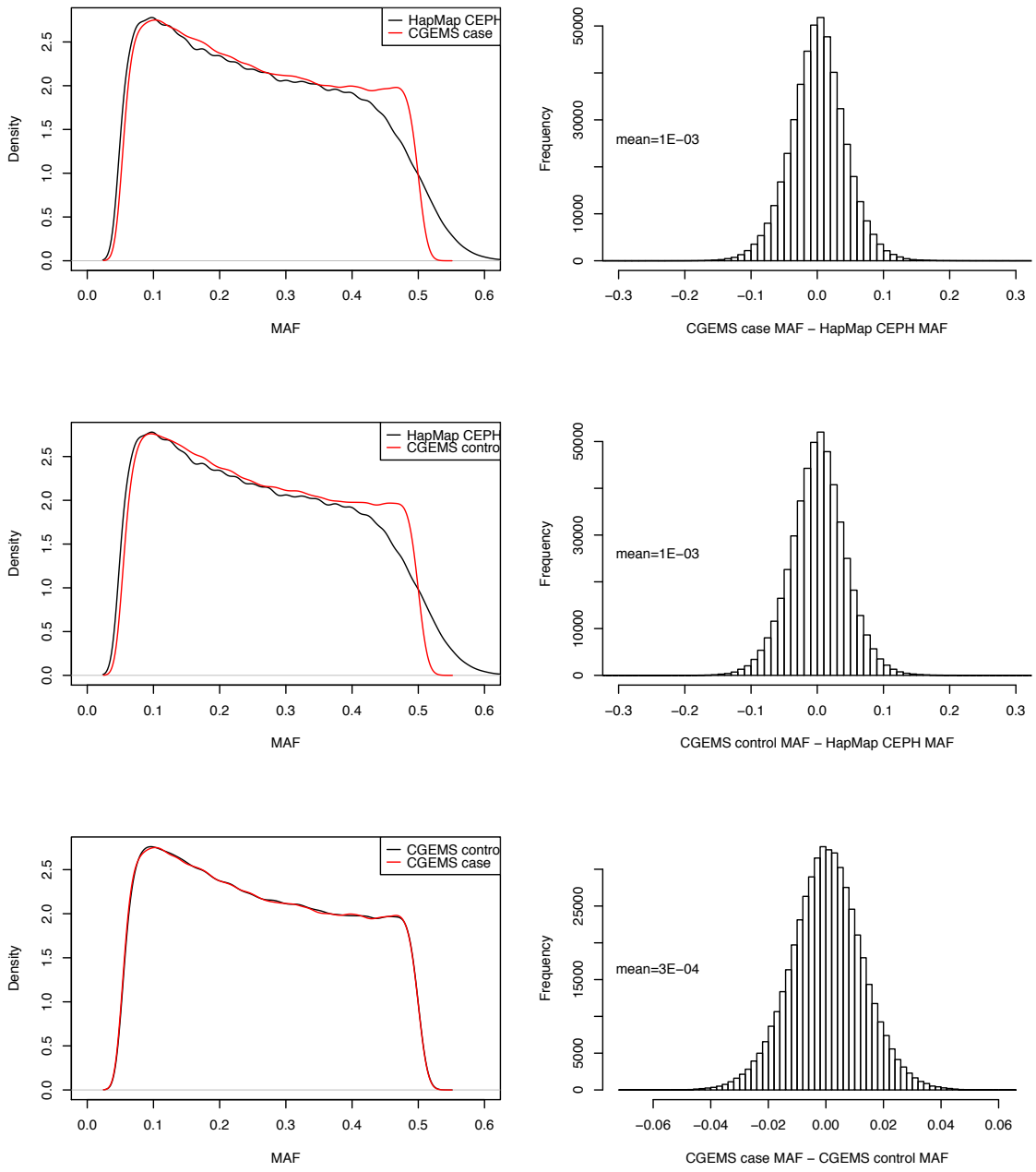

Figure 1: Distribution of minor allele frequencies (left) and differences (right) in CGEMS cases vs HapMap CEPHs (top), CGEMS controls vs HapMap CEPHs (center), and CGEMS cases vs CGEMS controls (bottom). Note that the distribution of MAF differences is much narrower when comparing CGEMS cases to controls (bottom) than when comparing either to HapMap CEPH. Only SNPs achieving frequencies of 0.05 or more were considered.

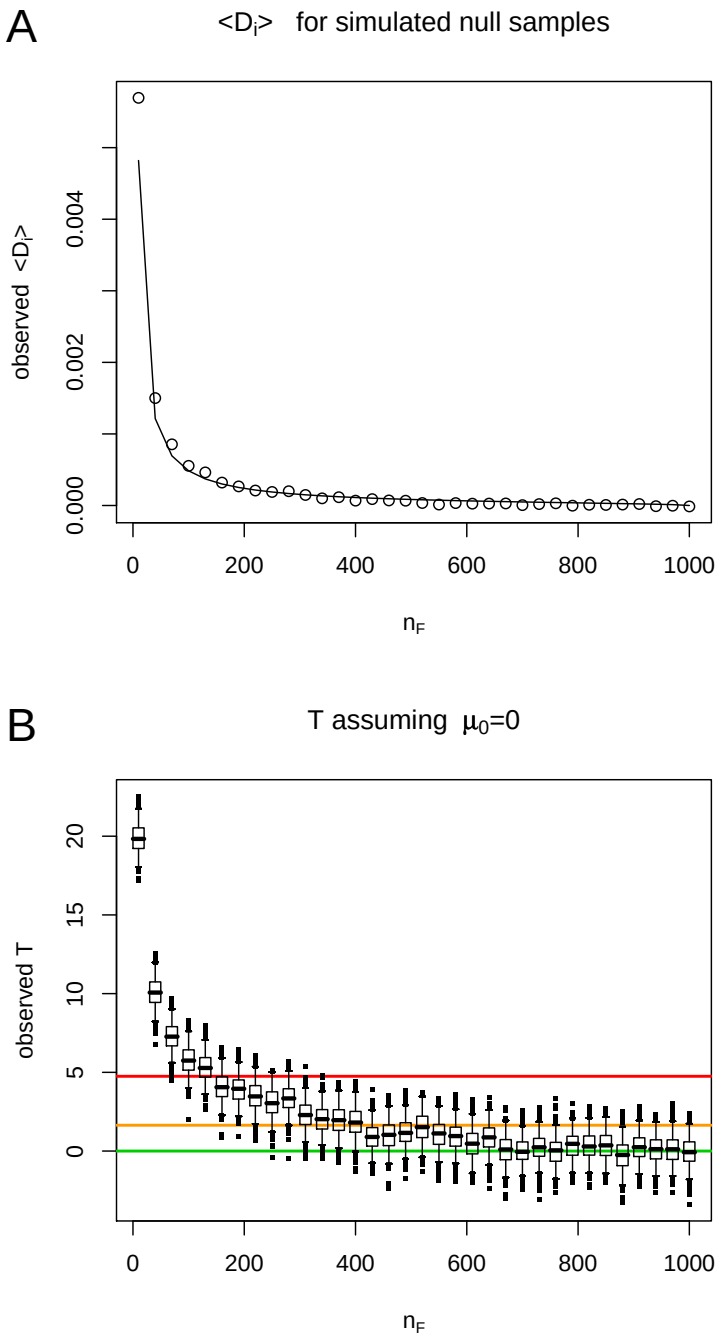

Figure 2: Observed $\langle D_i \rangle$ and T values for simulated data with varying sample sizes of n_F under the $\mu_0 = 0$ assumption. In A, open circles represent the average $\langle D_i \rangle$ for each simulation; the solid line is the theoretical $\langle D_i \rangle$ based on numerical integration of Eq. A-15. In B, boxplots of the observed Ts for each simulation are given assuming $\mu_0 = 0$; box boundaries correspond to the 0.25 and 0.75 quantiles, and whiskers indicate the 0.05 and 0.95 quantiles (T values outside those limits are shown as square points). Horizontal lines at $T = 0$ (green), $T = 1.64$ (corresponding to $\alpha = 0.05$, in amber), and $T = 4.75$ (corresponding to $\alpha = 10^{-6}$, in red) are shown for reference; note that for $n_F < 600$, at least 25% of null samples yield significant T at the nominal $\alpha = 0.05$.

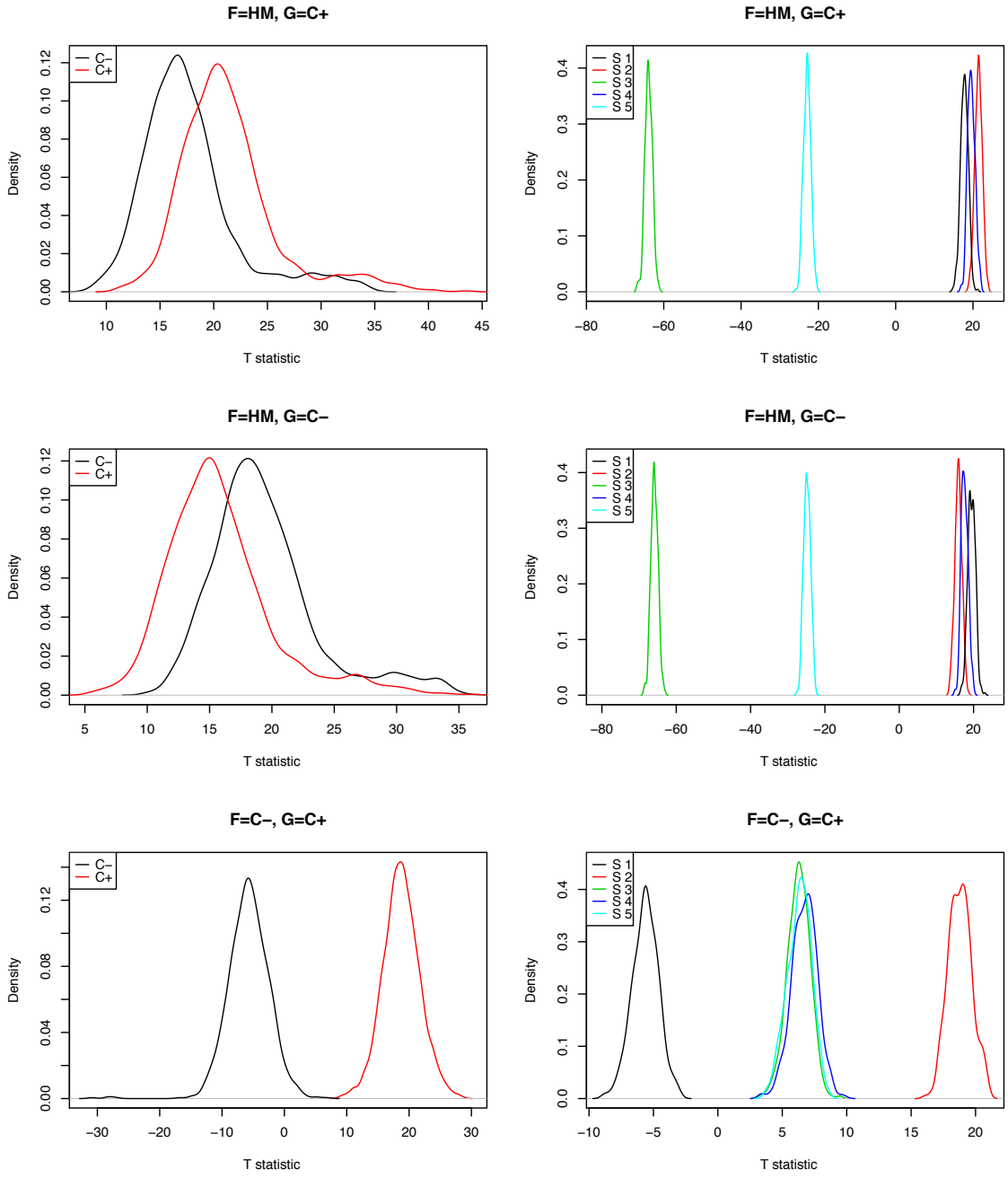

Figure 3: Distribution of T for real CGEMS samples (left column) and simulated samples S.1–S.5 (right column) using F/G pairs as follows: top, F = HapMap CEPHs, G = CGEMS cases; center, F = HapMap CEPHs, G = CGEMS controls; bottom, F = CGEMS controls, G = CGEMS cases. Only SNPs achieving frequencies of 0.05 or more were considered. Note that $|T| > 1.64$ is significant at the nominal $\alpha = 0.05$ level and $|T| > 4.75$ is significant at the nominal $\alpha = 10^{-6}$ under the putative null distribution.

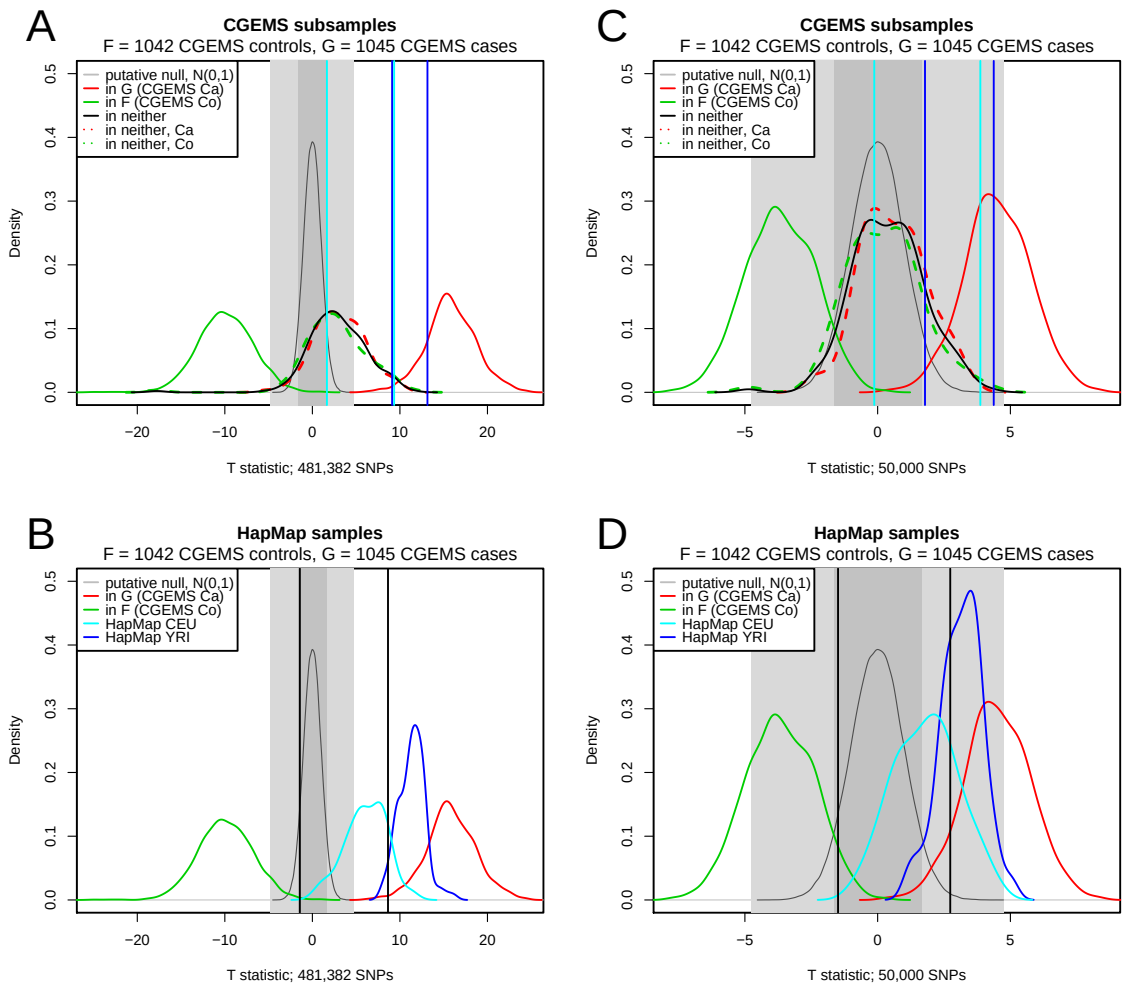

Figure 4: Comparison of T distributions for true positive and negative samples vs. putative null, starting with 481,382 SNPs in (A,B) and 50,000 SNPs in (C,D). In all plots, true positive F (1042 CGEMS controls) is shown as a solid green curve, true positive G (1045 CGEMS cases) is shown as a solid red curve, and the putative null $N(0,1)$ is given as a thin grey curve. The dark and light grey regions represent the areas for which the null hypothesis would be accepted at $\alpha = 0.05$ and $\alpha = 10^{-6}$, respectively. In plots (A,C), CGEMS test samples in neither F nor G (100 CGEMS cases and 100 CGEMS controls) are given by a heavy black curve. The CGEMS case and CGEMS control distributions within this group are shown as dashed red and green lines, respectively. In plots (B,D), T distributions are given for HapMap CEPHs (cyan) and YRIs (blue). Vertical lines mark the 0.05 and 0.95 quantiles of the negative CGEMS samples (black), HapMap CEPHs (cyan), and HapMap YRIs (blue).

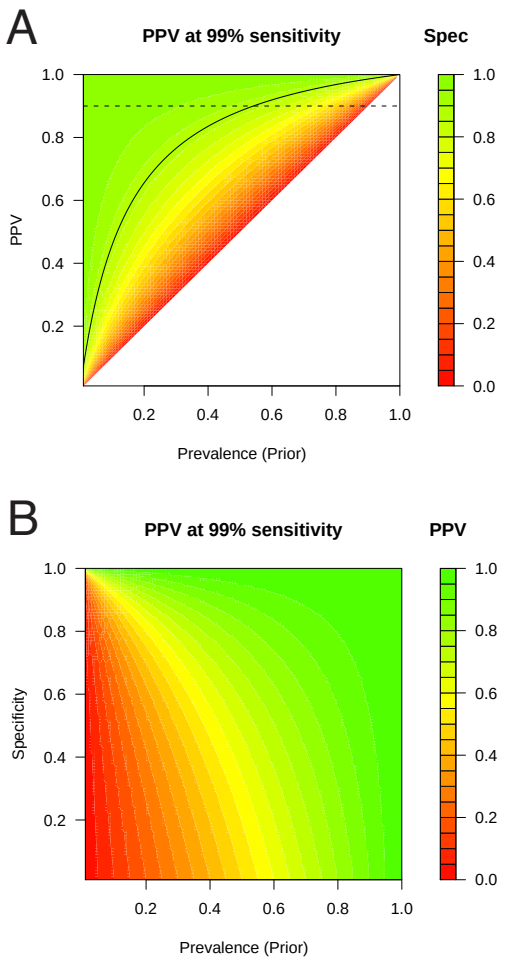

Figure 5: Positive predictive value (PPV) as a function of prevalence and specificity given 99% sensitivity. In (A), PPV is shown on the y axis and color corresponds to specificity. The black curve depicts the 87% sensitivity line—the best sensitivity obtained in the empirical tests in Tables 2, 3. In (B), PPV is shown by color, and the y axis corresponds to specificity.

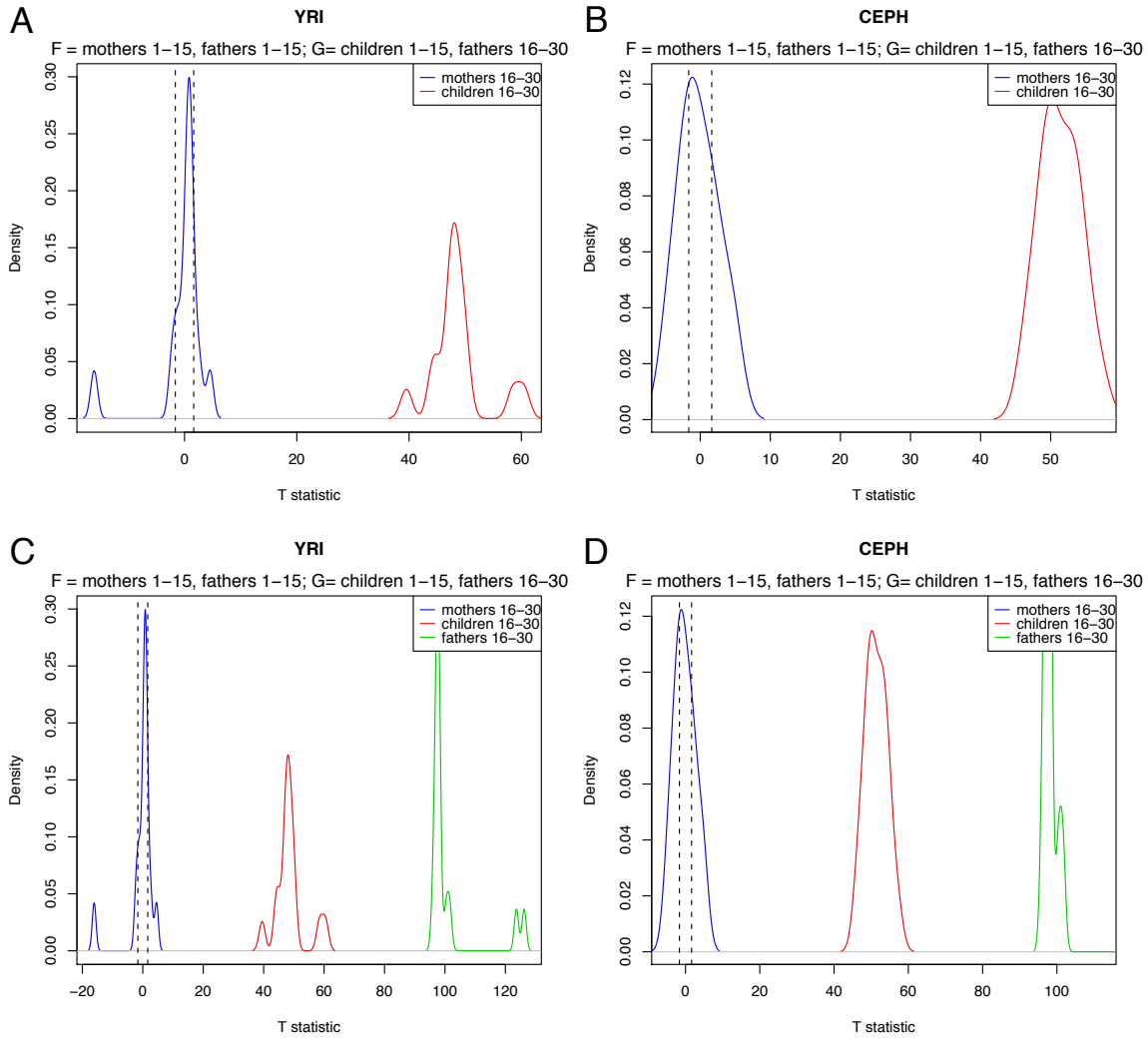

Figure 6: Distributions of T for out-of-group samples who are related (red line) and unrelated (blue line) to individuals in G for HapMap YRI (A) and HapMap CEPH (B) populations. (C) and (D) show the same distributions as (A) and (B) respectively, with the addition (green line) of individuals who are in G and unrelated to F (i.e., true positives). Dashed black lines indicate the T significance thresholds of ± 1.64 at nominal $\alpha = 0.05$.

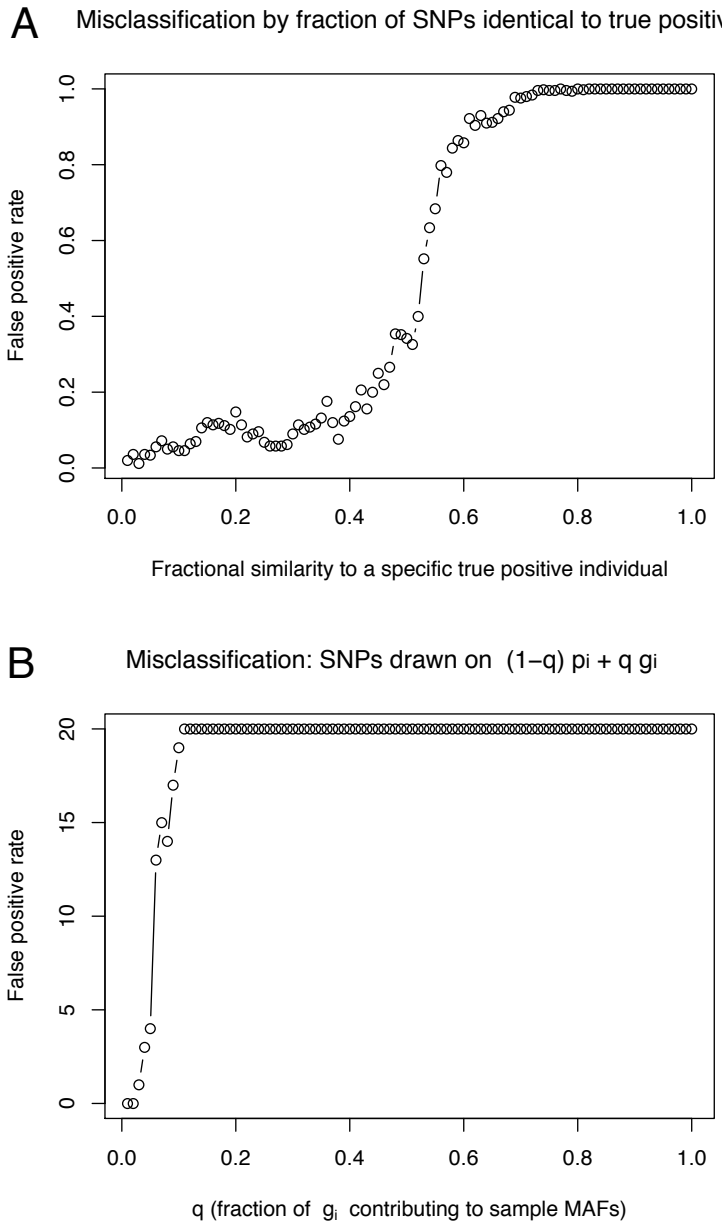

Figure 7: Misclassification rates for samples resembling true positives, as described in Sects. 2.3. In (A), samples were generated which had fractional genotype identity to a specific true positive; the false positive rate is given as a function of the pairwise similarity. In (B), samples drawn on a distribution that is a proportional mixture of g_i and the reference population MAFs; the false positive rate is given as a function of the proportion of g_i.